BIBECHANA
Vol. 23, No. 3, August 2026, 106–115

ISSN 2091-0762 (Print), 2382-5340 (Online)
Journal homepage: http://nepjol.info/index.php/BIBECHANA
Publisher: Dept. of Phys., Mahendra Morang A. M. Campus (Tribhuvan University), Biratnagar

MXene/Zn–graphene oxide hydrogels for enhanced energy storage and rate performance in pseudocapacitors

Maya Das[1], Anju Kumari Das[2], Shubha Sharma[1], Shova Neupane[1], Dipak Kumar Gupta[1*], Amar Prasad Yadav[1*]

[1]*Central Department of Chemistry, Tribhuvan University, Kirtipur, Nepal.*
[2]*Amrit Science Campus, Tribhuvan University, Kathmandu, Nepal.*

*Corresponding author: Email: deepakguptas2012@yahoo.com; amar.yadav@cdc.tu.edu.np

Abstract

The growing demand for high-performance supercapacitors has driven intensive research on two-dimensional (2D) nanoarchitectural materials. This study investigates MXene/Zinc-incorporated graphene oxide (MX:Zn–GO) hybrid hydrogels as pseudocapacitor electrodes to enhance energy storage and rate performance. MXene and Zn–GO were synthesized and assembled into three-dimensional hydrogels at room temperature with different zinc ratios. The morphology and composition were analyzed using scanning electron microscopy (SEM) and energy-dispersive X-ray spectroscopy (EDX), which confirmed distinct layered structures and homogeneous elemental distribution. The electrochemical performance was evaluated using cyclic voltammetry (CV), galvanostatic charge–discharge (GCD), and electrochemical impedance spectroscopy (EIS) in a three-electrode configuration. Among the tested compositions, the MX:Zn–GO (8:2) hydrogel composite, with a Zn:GO ratio of 2:1, exhibited the highest specific capacitance of 360 F g^{-1}*, an energy density of* 15.1 Whkg^{-1}*, a power density of* 101 Wkg^{-1}*, and* 93% *capacitance retention after 5000 charge–discharge cycles. These results demonstrate that composition-driven integration of MXene/Zinc-incorporated graphene oxide (MX:Zn–GO) within a hydrogel architecture offers a scalable route toward high-performance supercapacitor electrodes.*

Keywords
Synergistic nanocomposite, hydrogel electrode, 2D nanomaterials, energy storage, supercapacitors.

Article information
Manuscript received: February 21, 2026; Revised: June 28, 2026; Accepted: July 13, 2026
DOI: https://doi.org/10.3126/bibechana.v23i3.91135

1 Introduction

Two-dimensional transition metal carbides and nitrides (MXenes) have potential for supercapacitor applications due to their conductivity, layered structure, and abundant surface chemistry. From a wide range of reviews, it has been found that MXene derived from MAX phases, such as $Ti_3C_2T_x$

MXene, exhibits qualitative charge-transfer characteristics and configurable surface terminations that directly enhance its performance as an electrochemical energy storage device [1,2]. Moreover, reports on three-dimensional MXenes, such as hydrogels and aerogels, have shown further improved electrolyte ion accessibility due to reduced restacking problems [3,4]. Similarly, graphene oxide (GO) is a two-dimensional monolayer of graphene with a large surface area, functional groups, and a chemically active surface that enhances electrical conductivity. However, it cannot work alone as it shows a moderate conductivity, and its capabilities can be altered by reducing it with metals, such as zinc, in a versatile ratio of zinc. According to various studies, the reduced GO has enhanced electrochemical properties as compared with GO acting alone inside the fabricated material [5,6].

The concept of hybridization has been extensively investigated as an area in which MXene and graphene-based materials have been incorporated to aim for further increased electrochemical stability and capacitance. Reduced graphene oxide plays an important role in promoting hydrogel formation and integrity through structural engineering because of its large surface area and richness in oxygen-containing functional groups [7,8]. However, it does not show expected electrical conductivity, hence it should be combined with the materials having high electrical conductivity so that its useful characteristic features are valued as energy storage devices, such as supercapacitors. Several recent studies have mentioned the synergistic effects of MX:Zn-GO incorporation in lowering internal resistance and improving capacitance, along with charge transfer kinetics for which this combination is considered more effective than when they are used individually for the same purposes [4, 8]. In the field of electrochemistry, many studies related to the metal-assisted composition, such as MX:Zn-GO, have explained the great combination of this assembly as an electrochemical performance device if the interlayer spacing and charge transfer routes are controlled [9,10]. All studies have concluded that the logical design of MXene-Graphene Oxide hydrogel structures works effectively as high-performance supercapacitor electrodes.

In this study, MXene/Zn-graphene oxide hydrogel electrodes with optimized composition for pseudocapacitor applications are reported. The synthesis of $Ti_3C_2T_x$ MXene and Zn-incorporated GO at room temperature has been discussed. The layered shape and elemental distribution of the fabricated MXene were analyzed using SEM and EDX, which showed a specific capacitance of 244 $F\,g^{-1}$. SEM and EDX exhibited the distinctive nanosheet morphology of independently synthesized graphene oxide that showed a capacitance of 200 $F\,g^{-1}$. The hydrogel composite was synthesized by adding nano zinc to Graphene oxide in a 2:1 ratio at room temperature. The performance of MX:Zn-GO electrodes was measured in different ratios in which MX:Zn-GO (8:2) showed the highest specific capacitance of 360 $F\,g^{-1}$ and lowest impedance of 0.16 Ω while when the GO composition was slightly increased as in MX:Zn-GO (7:3) (340 $F\,g^{-1}$, 0.64 Ω) and MX:Zn-GO (6:4) (250 $F\,g^{-1}$, 0.67 Ω), the performances were relatively poor. This study highlighted the importance of MXene-based hydrogel for better ion transport and charge storage properties, ultimately leading to advanced supercapacitor applications [11,12].

2 Materials and Methods

2.1 Materials

Titanium Aluminum Carbide of high purity (MAX phase Ti_3AlC_2, 99.9% purity, Mol Wt.–194.6, APS: 500 nm TEM) was purchased from Nano Research, India. Similarly, Lithium Fluoride nanoparticles (99.9% purity, APS < 100 nm SEM, CAS No 7789-24-4, Mol Wt. 25.944) were bought from Nano Research Elements (India). Zinc nanoparticles (99.9% purity, 40–100 nm particle size) were purchased from Nano Research Elements (India). The rest of the chemicals, including potassium permanganate ($KMnO_4$, ≥ 99%), sulfuric acid (H_2SO_4, 95–98%), hydrogen peroxide (H_2O_2, 30%), hydrochloric acid (HCl, 37%), and potassium hydroxide (KOH, ≥ 85%) were of analytical grade and were from Thermo Fisher. Nickel foam (1.5 mm thickness, > 95% porosity), polyvinylidene fluoride (PVDF) binder, acetylene black, and N-methyl-2-pyrrolidone (NMP) solvent, which are the materials for the fabrication of electrodes, were purchased from Xiamen Tob Energy Technology, China. Double-distilled water was used to prepare all the solutions necessary for the study.

2.2 Synthesis of a few-layer MXene ($Ti_3C_2T_x$) aqueous dispersion from MAX phase (Ti_3AlC_2)

About 1.5 g of lithium fluoride (LiF, < 100 nm) and 60 mL of 6 M hydrochloric acid (HCl) were mixed in a plastic beaker and stirred continuously with a magnetic stirrer in a fume hood. Over a course of five minutes, 1.5 g of MAX phase titanium aluminum carbide (Ti_3AlC_2, APS ∼ 500 nm) was slowly added onto the mixture of LiF and HCl when all these chemicals were continuously stirred to ensure uniform dispersion [13,14]. Then, this mixture was allowed to react for 24 hours in a water bath at 45°C to ensure the selective etching of Aluminum

from the MAX phase. After 24 hours of reaction, the mixture was made free of acidic contaminants by repeatedly washing it with de-ionized water, centrifuging at 3500 rpm, and discarding the supernatant until the supernatant became neutral. The filtrate obtained after this purification showed a green tint, and further, in order to prevent restacking and oxidation, it was freeze-dried [13–15]. This final MXene product was then investigated using various characterization methods.

2.3 Synthesis of graphene oxide (GO) dispersion from graphite powder

Modified Hummers Method was used to synthesize Graphene Oxide (GO) from Graphite [16]. For this, 60 mL of concentrated sulfuric acid (H_2SO_4) was mixed with 1 g finely divided graphite, and the mixture was continuously stirred using magnetic stirring. In this mixture, 4 g of potassium permanganate ($KMnO_4$) was added very carefully by controlling the conditions so as not to exceed the temperature of 20°C to yield a viscous green paste. The mixture was left to cool down and then diluted slowly by adding 200 mL of crushed ice to prevent any unnecessary reactions. After this, the oxidation reactions of the mixture ceased by adding 3 mL of 30% pure hydrogen peroxide (H_2O_2), where the colour of the mixture changed from dark brown to light yellow. Then, this final product was subjected to multiple centrifugation cycles (3500 rpm) along with alternatively washing it with 10% hydrochloric acid (HCl) and deionized water [5, 17, 18].

2.4 Fabrication of MXene/Zn-graphene oxide hybrid hydrogels (MX:Zn-GO)

MXene/Zn-graphene Oxide hybrid hydrogels (MX:Zn-GO) with a variation in MXene loadings (ranging from 80 wt% to 60 wt%), individually synthesized in an aqueous dispersion of MXene and GO that were combined in appropriate ratios. Then, nanometer-sized nano-zinc was incorporated into the MXene/GO combination at a Zn-to-GO mass ratio of 2:1. This mixture was manually agitated for some durations, which converted the dispersion into a cohesive, clay-like mass.

The paste of the mixture inside the cylindrical glass mold was allowed to stand for 12 h for the formation of a bulk cylindrical hydrogel. Now these hydrogels with required geometrical structures were produced by casting the paste into plastic molds. In order to remove unused Zn particles and by-products obtained by oxidation during gelation, the fabricated MGH was placed in a 10% hydrochloric acid (HCl) solution. This acid-treated hydrogel was dialyzed in deionized water for long durations to remove excess acid and Zn ions.

Various hybrid hydrogels with different MXene-to-GO weight ratios were synthesized by altering the relative contents of MXene and GO, however, keeping the overall concentration of the two components at 10 mg mL^{-1}. The samples of this material were identified as MGH4:1 (80 wt% MXene), MGH7:3 (70 wt%), and MGH3:2 (60 wt%) based on the ratio of MXene used [19].

2.5 Fabrication of the working electrode

The working electrode was fabricated by coating the mixture of active material onto a previously cleaned nickel foil substrate (1 × 1 cm^2), Figure 1. For this, the electrode ink was made by homogeneously mixing 80 wt% active material, 10 wt% polyvinylidene fluoride (PVDF) binder, and 10 wt% conductive carbon black in an agate mortar. The uniform slurry was created by adding a controlled amount of N-methyl-2-pyrrolidone (NMP) to the mixture slowly. Then the whole mixture was ground for 15 minutes and sonicated to ensure complete dispersion.

Then, the obtained homogeneous slurry was carefully coated onto the nickel foam current collector in a balanced manner for even distribution by using a micropipette. After this, the prepared electrode was compressed at 10 MPa using a hydraulic pressure and left to dry at 60°C for 12 hours in a vacuum oven so as to make it dry and remove excess solvent. The compression was done to enhance electrode integrity and interfacial contact.

Before electrochemical testing of the fabricated electrode, it was taken for active material mass loading determination using a microbalance (resolution: 0.01 mg). Then the electrode was immersed in 6 M potassium hydroxide (KOH) solution so that it became completely wet before being used as an electrode in a three-electrode cell for electrochemical analysis.

2.6 Materials characterization

The prepared nanoparticles were subjected to morphological and electrochemical characterizations using different techniques. Nanoparticles were sonicated and spread over a copper grid coated with carbon tape. Then, the grid was kept in a desiccator, and nitrogen gas was passed for 24 hours. It was dried at room temperature (RT) and subjected to morphological analysis using a field-emission scanning electron microscope (FEI Quanta FEG 200F) with a resolution of ∼ 1.2 nm and magnification up

to 10^5. This system can be used for high-vacuum (conductors), low-vacuum (insulators), and ESEM (biospecimens) operations. The composition of elements present in the nanoparticles was determined by using the integrated EDX and WDS detectors.

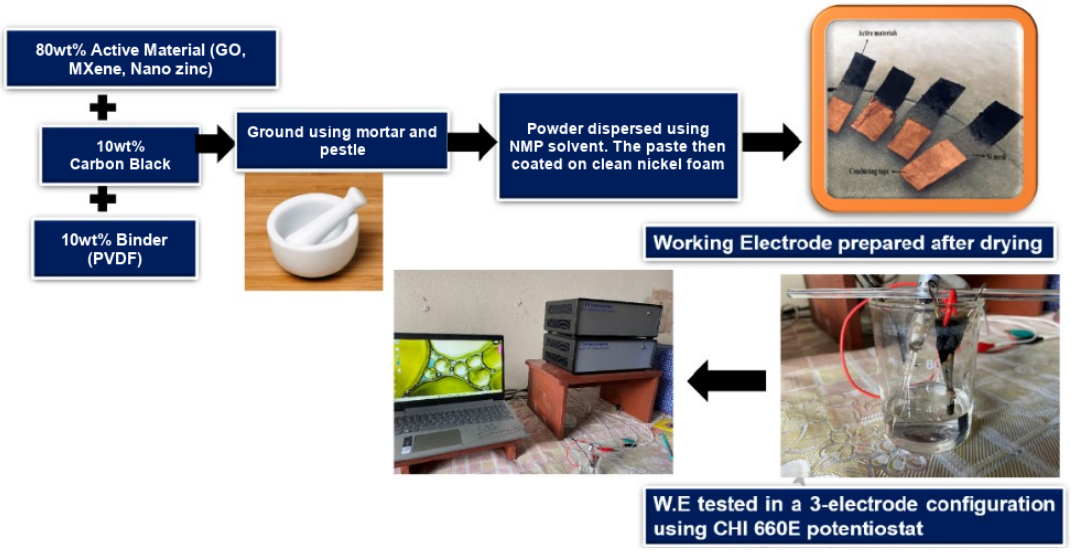

Figure 1: Schematic illustration of electrode preparation by the Drop Casting Method.

Electrochemical characterization of the material was performed using a potentiostat/galvanostat system (CH Instruments 660E). In a three-electrode setup, the platinum wire served as the counter electrode, the saturated calomel electrode (SCE) as the reference electrode, and the nickel foam coated with the sample as the working electrode. The open-circuit potential (OCP) was measured for 10 minutes before each measurement. Cyclic voltammetry (CV) was then performed in 6 M KOH to optimize and assess the material's redox system within a 0 to 0.55 V potential window. Supercapacitor behavior was also examined by CV. Galvanostatic charge-discharge (GCD) was carried out to determine specific capacitance and energy density. Electrochemical impedance spectroscopy (EIS) was performed to study kinetics and charge transfer. Specific capacitance, energy density, and power density were calculated using Equations (1)-(3), expressed below

$$\mathrm{SC} = \frac{I \times \Delta t}{\Delta V \times m} \tag{1}$$

$$E = \frac{\mathrm{SC} \times \Delta V^2}{8 \times 3.6} \tag{2}$$

$$P = \frac{3600 \times E}{\Delta t} \tag{3}$$

$\mathrm{Wh\,kg^{-1}}$ is the unit of energy density (E), whereas $\mathrm{W\,kg^{-1}}$ is the unit of power density (P). The capacitance retention was calculated using Equation (4), given below

$$\text{Capacitance retention } (\%) = \frac{\text{Final capacitance}}{\text{Initial capacitance}} \times 100\% \tag{4}$$

3 Results and discussion

3.1 Scanning electron microscopy (SEM) analysis and energy dispersive X-ray (EDX)

According to Scanning electron microscopy (SEM) analysis, the synthesized Graphene oxide and MXene showed varied morphologies as displayed in Figure 2(a), as the thin, crumpled, and wrinkled sheet-like structures were determined, which is due to the oxidation-induced lattice distortion and expanded interlayer spacing [20]. This structure is a foundation for inhibiting sheet restacking and increasing accessible surface area, finally promoting electrolyte penetration and ion diffusion. Many reports have mentioned the importance of these characteristics as an aid to upgrade charge storage behavior in an electrochemical energy storage system. Conversely, the image of MXene as shown in Figure 2(b) exhibited its unique layered and plate-like flakes along with smooth basal planes, which were divided by $Ti_3C_2T_x$ structures.

The two-dimensional structure of synthesized MXene is responsible for continuous electron transport pathways and helps to promote ion interaction,

which are the mandatory features for an electrochemical system [3]. Moreover, this stacked yet accessible layered structure aids in efficient ion intercalation and deintercalation during electrochemical cycling, which is the most important characteristic for facilitating high-rate performance. Furthermore, in a hybrid electrode system, MXene sheets having a wide range of interlayer spacing are found to be effective conductive frameworks, enhancing the electrochemical stability and capacitance retention [21].

The EDX spectra of graphene oxide (GO) and MXene (MX) are shown in Figure 2, displaying distinctive variations in their morphology and elemental composition. According to the EDX spectrum of GO, carbon (C) and oxygen (O) are the two predominant elements with a significant amount of oxygen content, which is due to the presence of several oxygen-containing functional groups that are added for the oxidation of graphite. Small amounts of sulfur (S) and nitrogen (N) present in its structure are due to residual reagents or surface functionalization during chemical synthesis, which are the common elements for the GO prepared chemically in the lab. The oxygen-rich structure facilitates surface polarity and electrolyte wettability, and ultimately promotes ion transport in electrochemical systems [15]. Conversely, the EDX analysis of MXene showed a strong titanium (Ti) signal along with carbon (C), indicating the synthesis of $Ti_3C_2T_x$-type MXene. A small amount of aluminum (Al) and chlorine (Cl) was detected, with their peaks revealing the partial elimination of the parent MAX phase and residual etching by-products, which is a common detection in MXene synthesized using selective etching routes. According to the SEM image, MXene showed a layered and stacked flake-like morphology along with two-dimensional carbide structures [6]. Overall, the variations in elemental compositions and layered structures of GO and MXene as provided by SEM-EDX analysis revealed their roles for aiding each other in hybrid electrode systems, for which GO facilitates surface functionality, and MXene promotes high electrical conductivity and structural stability [15, 21].

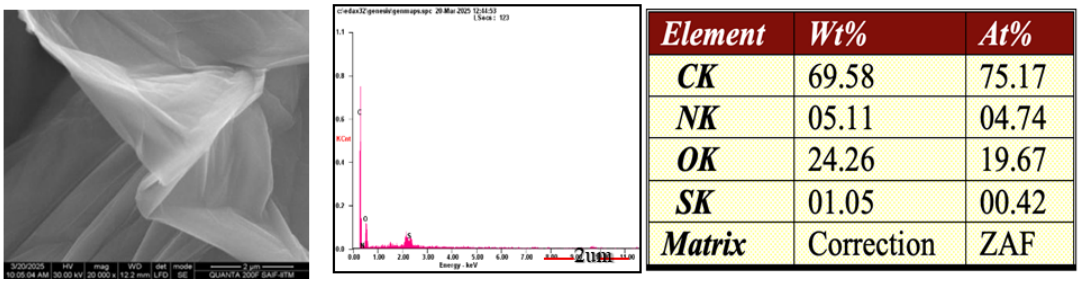

Element	Wt%	At%
CK	69.58	75.17
NK	05.11	04.74
OK	24.26	19.67
SK	01.05	00.42
Matrix	Correction	ZAF

(a)

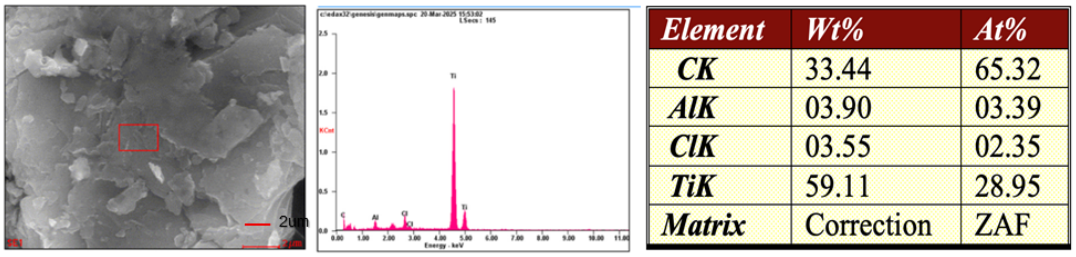

Element	Wt%	At%
CK	33.44	65.32
AlK	03.90	03.39
ClK	03.55	02.35
TiK	59.11	28.95
Matrix	Correction	ZAF

(b)

Figure 2: EDX and SEM, which demonstrates the variations in elemental composition and structure between (a) Graphene oxide (GO) (b) MXene (MX).

3.2 Electrochemical Characterization

3.2.1 Cyclic Voltammetry (CV)

The cyclic voltammetry of graphene oxide (GO), as shown in Figure 3(a), reveals low current density with less enclosed CV areas in different scan rates due to the fact of oxidation of graphene oxide, which retains the peak, decreasing the conductivity, affecting charge transport kinetics. Figure 3(b) shows the CV of MXene (MX), which revealed the high current density with enclosed surface coverage in CV at different scan rates with an intense peak, which increased the conductivity with excellent charge transport kinetics.

Electrochemical responses depended on the composition of MX:Zn-GO composite hydrogels as revealed by the cyclic voltammetry (CV) curves. Fig-

ure 3(c) shows the CV of the composites performed at 10 mV scan rates. Out of all the different composites, the MX:Zn-GO (8:2) hydrogel (Figure 3(d)) displayed the highest current response and larger area of enclosed CV, depicting the efficient charge storage as provided by the highly conductive MXene sheets [15]. Similarly, the composite, MX:Zn-GO (7:3), demonstrates definitive characteristics related to its redox behaviour along with its good shape retention when the scan was kept higher; however, its current response was not as supportive as expected [22]. Conversely, the MX:Zn-GO (6:4) composite shows lower current response in comparison with other composites, which is due to an increment in GO content, allowing for incomplete reduction in electrical conductivity. Overall, MXene-rich hydrogels promote effective electrochemical kinetics and rate capability; however, GO contributes to structural stability and electrolyte wettability in hybrid electrochemical system [20,23,24].

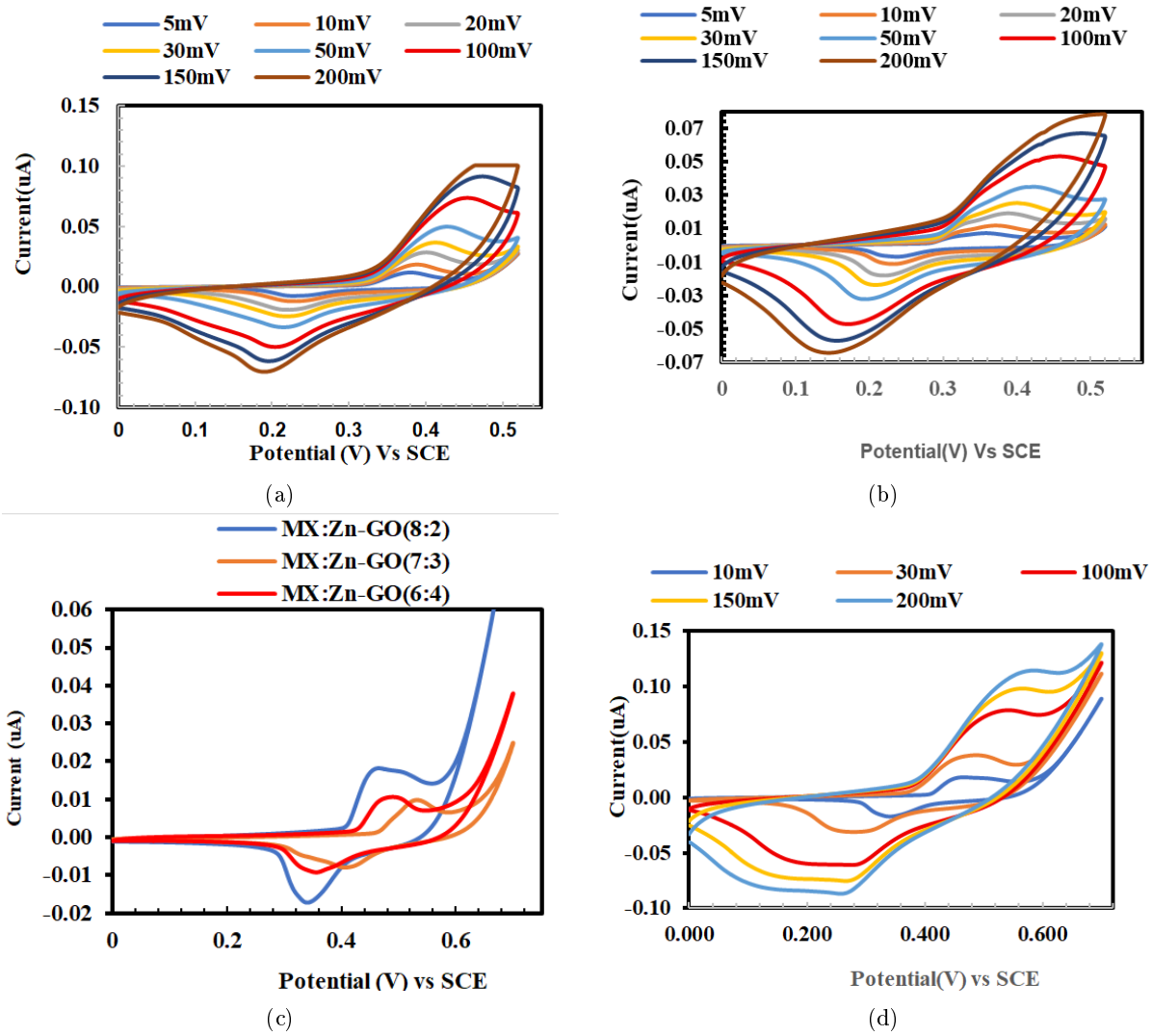

Figure 3: (a) CV of graphene oxide (GO), (b) CV of MXene (MX), (c) CV of MX:Zn–GO in different ratios at 10 mV, and (d) CV of MX:Zn–GO (8:2).

3.2.2 Galvanostatic charge-discharge (GCD)

The galvanostatic charge-discharge (GCD) is shown in Figure 4. It reveals the behavior of GO, MXene, and MX:Zn-GO composites with different compositions. Figure 4(a) shows a shorter discharge time and a larger voltage drop due to the limited conductivity and poor ion transport of graphene oxide. Figure 4(b) shows a longer discharge time and good metallic conductivity of MXene. However, at higher current density, due to restacking of the layer, its performance deteriorates with a decrease in performance and ion accessibility between the MXene layers.

Among the various samples (Figure 4(c)) of composites synthesized, the MX:Zn-GO (8:2) electrode

shows the longest discharge time, demonstrating the optimal synergistic function of conductive MXene layers and ion-accessible GO sheets such that an increase in GO content facilitates the higher internal resistance and decreased discharge durations as a result of restacking and decreased electron transport pathways [13]. Figure 4(d) shows the MX:Zn-GO (8:2) electrode, with stable capacitive behavior and combined EDLC and pseudocapacitive behavior. The gradual decrease in discharge time at high current density shows low ion diffusion, a smaller IR drop shows lower internal resistance, and faster ion transport kinetics. Overall, the GCD curves, which directly depend upon the compositions of the materials, mention the balanced ion diffusion, charge transfer efficiency, and structural integrity in the MXene/Zn-GO hybrid electrochemical system [15].

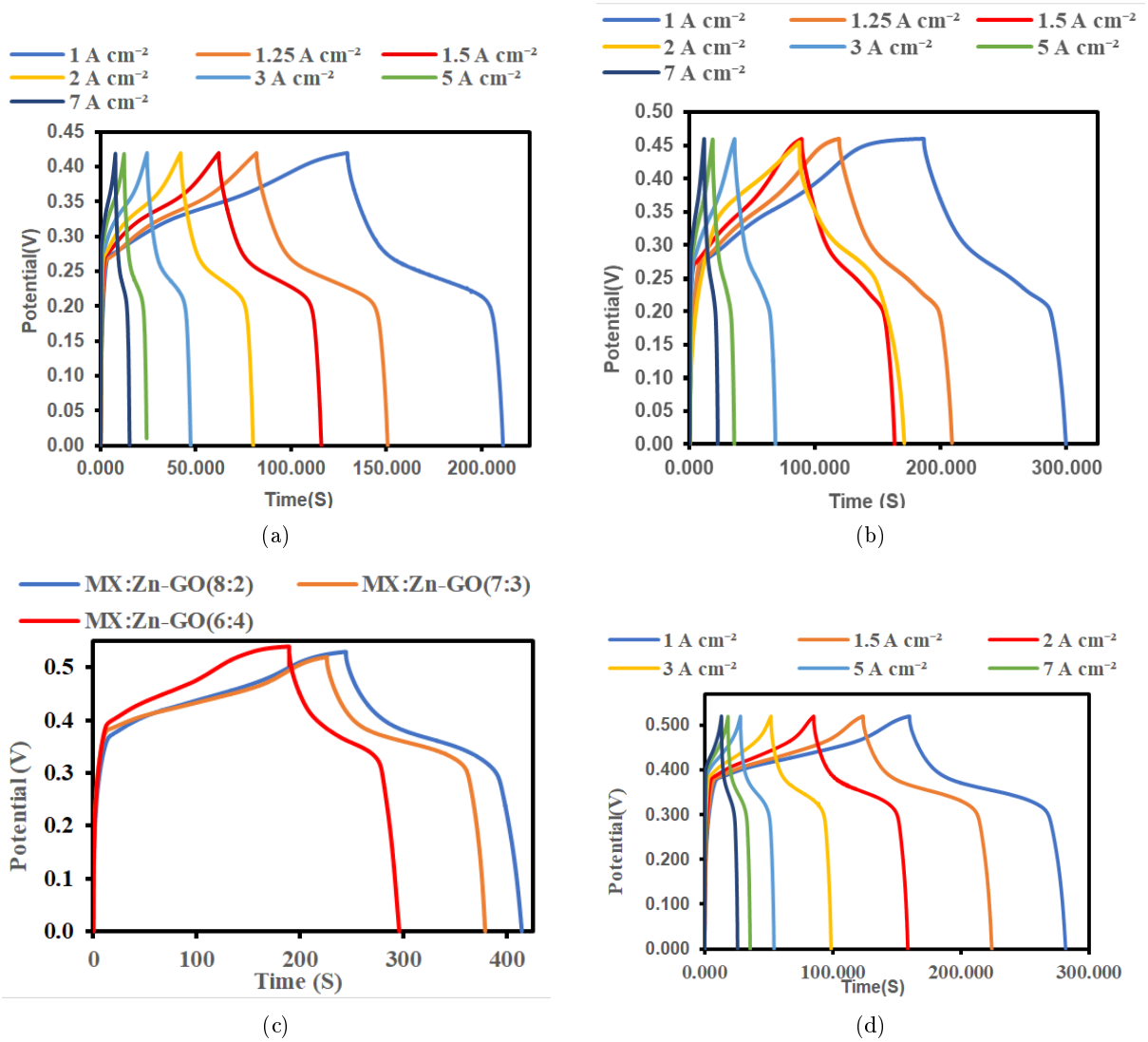

Figure 4: (a) GCD of graphene oxide (GO), (b) GCD of MXene (MX), (c) GCD of MX:Zn–GO in different ratios at 1 Acm^{-2}, and (d) GCD of MX:Zn–GO (8:2).

3.2.3 Electrochemical Impedance Spectroscopy (EIS)

Figure 5 shows the Nyquist plots of the MXene/Zn-GO hydrogels, which show a modest intercept in the high-frequency area along with a line inclined in the low-frequency area, depicting low equivalent series resistance and dominating capacitive behavior. Comparatively, the MX:Zn-GO (8:2) composite displays the real-axis intercept and the steepest low-frequency slope, revealing quicker charge transfer and better ion diffusion due to a well-connected conductive network. Similarly, the increase of GO content in the MX:Zn-GO (6:4) sample composite shows greater impedance due to a decrease in electronic pathways and incomplete restacking, which disturbs the charge transport. The near-vertical Warburg region demonstrates productive

electrolyte penetration and synergistic interplay of MXene conductivity and GO surface functionality [25].

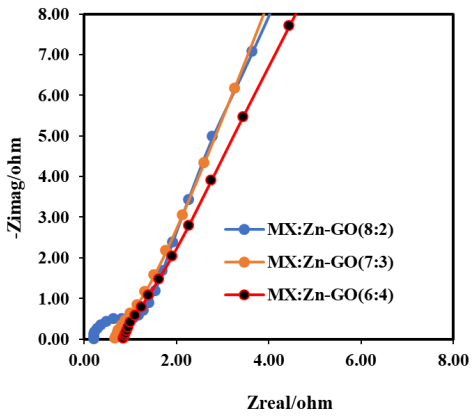

Figure 5: EIS of MX:Zn–GO (8:2), MX:Zn–GO (7:3), MX:Zn–GO (6:4).

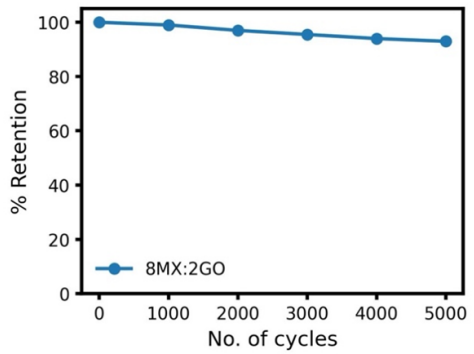

Figure 6: Capacitance retention for 5000 cycles of 8MX:2GO.

Electrochemical analysis of the synthesized materials showed the synergistic benefits of the MXene/Zn-GO hybrid system. The MX:Zn-GO (8:2) electrode shows the highest specific capacitance (360 $F\,g^{-1}$) and specific capacity (55.0 $mAh\,g^{-1}$) inside a good retention potential window of 0.55 V, which aids in enhancing energy and power densities [20] (Figure 6). Previously, two different studies showed the capacitance of 357 $F\,g^{-1}$, where one of the studies used the MXene/GO hybrid hydrogel and the other used integrated MXene/rGO (reduced graphene oxide) [6, 19]. The increase in capacitance value to 360 $F\,g^{-1}$ is due to efficient charge transport as provided by conductive MXene sheets combined with ion-accessible functional groups of GO [26,27]. This enhancement of the capacitance value can be viewed as a progressive approach, as some reports suggest a capacitance of 335 $C\,g^{-1}$ where MXene/rGO was used as a primary material [21]. In MX:Zn-GO (7:3) and MX:Zn-GO (6:4), where GO content is increased, capacitance is decreased, which is a result of increased interfacial resistance, even though the electrolyte wettability is improved [28–31]. Hence, the superior structural integrity and electrochemical durability of optimized MX:Zn-GO (8:2) electrode show $\sim 93\%$ capacitance retention after 5000 cycles, confirming excellent cyclic stability. At a current density of 1 $A\,cm^{-2}$, the optimized electrode delivered a power density of 101 $W\,kg^{-1}$ (Equation 3).

Table 1: Electrochemical performance of electrodes

S.N.	Electrode	Sp. Cap. ($F\,g^{-1}$)	Pot. Win. (V)	Sp. Cap. ($mAh\,g^{-1}$)	E. Dens. ($Wh\,kg^{-1}$)	P. Dens. ($W\,kg^{-1}$)
1	8MX:2GO	360	0.55	55.0	15.1	101
2	7MX:3GO	340	0.55	51.9	14.3	96
3	6MX:4GO	250	0.55	38.2	10.5	70
4	MXene	244	0.45	30.5	6.86	46
5	GO	200	0.42	23.3	4.9	33

4 Conclusion

This study presents a novel, scalable fabrication route for high performance energy storage through a synergistic MXene/Zn-graphene oxide (GO) hybrid hydrogel electrode. Among all the composites, the optimized MX:Zn-GO (8:2) composition shows an efficient and great electrochemical performance that successfully helps in providing a high specific capacitance of 360 $F\,g^{-1}$, promoted energy density of 15.1 $Wh\,kg^{-1}$, and brilliant cycling stability with over 93% capacitance retention after 5000 cycles. The synergistic functions of MXene and GO improved the electrochemical behavior, for which MXene demonstrated continuous conductive networks and pseudocapacitive activity, and GO reduced nanosheet restacking effectively and upgraded electrolyte accessibility. Similarly, the SEM

analysis displays a well-interconnected, porous, and layered hydrogel structure that promotes efficient ion transport, along with the EDX, which shows the homogeneous distribution of elements for the successful incorporation of MXene and GO inside this hybrid electrochemical system. Furthermore, the electrochemical impedance analysis confirms the structural benefits by demonstrating a decrease in charge-transfer resistance and upgraded ion diffusion kinetics in the optimized electrode. The novelty of this work lies in the room-temperature, Zinc-assisted assembly of $Ti_3C_2T_x$ MXene and Zinc-GO into a three-dimensional hydrogel that simultaneously optimizes interlayer spacing, charge transfer pathways, and electrolyte accessibility without high temperature or binder. The optimized MX:Zn-GO (8:2) hydrogel delivers competitive specific capacitance, energy density, and cycling stability, establishing a practical and scalable electrode platform for next-generation pseudocapacitors.

Conflict of interest

The authors declare that there are no financial or personal relationships that could have influenced the outcome of this research. The work received financial support from the University Grants Commission (UGC), Nepal.

Acknowledgments

The Indian Institute of Technology Madras (IIT Madras) is acknowledged for providing SEM-EDX of the materials. M. Das is thankful to the University Grants Commission, Sanothimi, Nepal, for the Ph.D. fellowship (UGC Award No PhD-79/80-S&T-05). The authors also extend gratitude to the Central Department of Botany, Tribhuvan University, for facilitating the freeze-drying of the samples.

Authors' contributions

MD: Writing original draft, investigation, formal analysis and data curation. AKD: Investigation and data curation. SS: Experimentation and data curation. SN: Writing review & editing, supervision and project administration. DKG: Writing review & editing, supervision and formal analysis. APY: Writing, review & editing, supervision and conceptualization.

References

[1] Ajmal Z, Qadeer A, Singh K, Mahmud AA, Lakhan MN, Pradeep H, et al. A comprehensive review on MXenes for various applications. Applied Energy. 2025;397:126136.

[2] Li S, Wang Y, Zhang X, Xu J. Directional fabrication of an ultra-light and porous bacterial nanocellulose/MXene aerogel. Carbohydrate Polymers. 2025;324:120549.

[3] Bansal S, Chaudhary P, Sharma BB, Saini S, Joshi A. Review of MXenes and their composites for energy storage applications. Journal of Energy Storage. 2024;87:111420.

[4] Gao T, Lai CW, Rangappa SM, Siengchin S, Gapsari F, Li Y, et al. MXene-based materials for supercapacitors: Trends and opportunities. Journal of Materials Science: Materials in Electronics. 2025;36:1877.

[5] Mushahary N, Sarkar A, Basumatary F, Brahma S, Das B, Basumatary S. Recent developments on graphene oxide and its composite materials. Surfaces and Interfaces. 2024;15:100225.

[6] Sahoo PK, Kumar N, Jena A, Mishra S, Lee CP, Lee SY, et al. Recent progress in graphene and its derived hybrid materials for high-performance supercapacitors. RSC Advances. 2024;14:1284-303.

[7] Xu T, Song Q, Liu K, Liu H, Pan J, Liu W, et al. Nanocellulose-assisted construction of multifunctional MXene-based aerogels. Nano-Micro Letters. 2023;15:98.

[8] Zhan M, Xu M, Lin W, He H, He C. Graphene oxide research: Current developments and future directions. Nanomaterials. 2025;15:507.

[9] Gogotsi Y, Anasori B. The Rise of MXenes. ACS Nano. 2019;13:8491-4.

[10] Ji P, Liu L, Deng Y, Luo Y, Cao Y, Li B, et al. Three-dimensional hierarchical porous MXene aerogel with outstanding rate performance for flexible supercapacitors. Journal of Energy Storage. 2024;93:112194.

[11] Sun Y, Yang X, Ding R, Hong SY, Lee J, An Z, et al. Super-elastic and mechanically durable MXene-based nanocomposite aerogels. Nano Research. 2023;16:8025-35.

[12] Suresh S, Krishnan VG, Dasgupta D. Directional-freezing-enabled MXene orientation toward anisotropic PVDF/MXene aerogels. ACS Applied Materials & Interfaces. 2023;15:49567-82.

[13] Rundla A, Priyanka, Kumar B, Tripathi P, Kumar P, Singh K. $Ti_3C_2T_x$ MXene@rGO composite electrodes for high-performance supercapacitors. Journal of Power Sources. 2025;632:236408.

[14] Bao W, Tang X, Guo X, Choi S, Wang C, Gogotsi Y, et al. Porous cryo-dried MXene for efficient capacitive deionization. Joule. 2018;2:778-87.

[15] Jia XT, Xing HW, Cheng XW, Zhang ZH, Wang Q, Zhou JZ, et al. Two-dimensional nanostructured $Ti_3C_2T_x$ MXene for ceramic materials: Preparation and applications. Nanomaterials. 2025;15:204.

[16] Marcano DC, Kosynkin DV, Berlin JM, Sinitskii A, Sun Z, Slesarev A, et al. Improved synthesis of graphene oxide. ACS Nano. 2010;4:4806-14.

[17] Adetayo K, Runsewe D. A review of graphene oxide morphology and properties. Open Journal of Composite Materials. 2019;9:207-29.

[18] Sikdar A, Majumdar P, Dutta M, Borah S, Kim SO, Maiti UN. Ultra-large area graphene hybrid hydrogel for customized performance supercapacitors. Electrochimica Acta. 2020:135492.

[19] Sikdar A, Dutta P, Deb SK, Majumdar A, Padma N, Ghosh S, et al. Spontaneous three-dimensional self-assembly of MXene and graphene for impressive energy and rate performance pseudocapacitors. Electrochimica Acta. 2021;391:138959.

[20] Kaftelen-Odabaşı H. Evaluation of morphological, structural, thermal, electrical, and chemical composition properties of graphene oxide and reduced graphene oxide. Carbon Trends. 2024;17:100429.

[21] Karthikeyan S, Arumugam J, Suresh A, Raj AD. Enhanced capacitance and rate performance of $Ti_3C_2T_x$/RGO electrodes for asymmetric supercapacitors. Journal of Porous Materials. 2025;32:1961-73.

[22] Siddu PSNK, Jeong SM, Rout CS. MXene-carbon based hybrid materials for supercapacitor applications. Energy Advances. 2024;3:341-65.

[23] Zhang S, Liu X, He J, Yan W, Xu H, Qiu Z. 3D hierarchical $Ti_3C_2T_x$@$NiCo_2S_4$-reduced graphene oxide hydrogel with high cycle stability for battery-type Zn-ion energy storage device. Journal of Power Sources. 2026;677:240006.

[24] Fadavi P, Mehrpooya M, Ganjali MR. Dual metal deposited MXene-covalent organic framework hydrogel for supercapacitor and water splitting applications. Journal of Power Sources. 2026;678:240121.

[25] Yuan Z, Zhang W, Wang J, Liu Y, Zhao H. Preparation of $Ti_3C_2T_x$ MXene/GO composites with enhanced electrochemical performance for lithium-ion capacitors. Russian Journal of Electrochemistry. 2024;60:1153-62.

[26] Yang C, Zhang X, Wang T, Araby S, Wang CH. Highly porous and compressible MXene aerogels fabricated by freeze-drying for high-performance supercapacitors. Chemical Engineering Journal. 2022;430:132745.

[27] Baimenov A, Daulbayev C, Poulopoulos SG, Mochalin VN. MXene filled hydrogel and aerogel composites. Materials Today. 2024;78:75-91.

[28] Kiran H, Ali ABM, Ashraf R, Tahir MB, Nasir M, Hasnain N, et al. Comparative study of $Ti_3C_2T_x$ MXene synthesized via HF and LiF-HCl etching. Journal of Inorganic and Organometallic Polymers and Materials. 2025;35:1-17.

[29] Patro A, Rajbhar M, Patra A, Chatterjee S, Rout C, Dhal S. Augmented electrochemical properties of manganese oxide nanorods. Journal of Alloys and Compounds. 2023;960:170441.

[30] Soomro RA, Zhang P, Fan B, Wei Y, Xu B. Progression in the oxidation stability of MXenes. Nano-Micro Letters. 2023;15:108.

[31] Suganthi S, Ahmad K, Oh TH. Progress in MXenes and their composites as electrode materials for electrochemical sensing and energy applications. Molecules. 2024;29:5233.